Supporting Information

Bepperling et al. 10.1073/pnas.1209565109

SI Materials and Methods

Preparation of Genomic DNA from *Deinococcus radiodurans*. Cells were grown in 100 mL TGY (1% bactotryptone, 0.5% yeast extract, and 0.1% glucose) for 72 h at 30 °C, harvested by centrifugation (5 min, 4,000 × *g*), washed with 1 mL water and 1 mL ethanol, and incubated in 400 μL TE [10 mM Tris·HCl (pH 8.0), 1 mM EDTA] containing 50 μg lysozyme for 30 min at 25 °C. Phenol/chloroform/isoamylalcohol (25:24:1; 800 μL) were added, and after centrifugation (2 min, 13,000 × *g*), the supernatant was transferred to a new tube. This step was repeated. The resulting supernatant was precipitated with 100% ethanol and centrifuged (10 min, 13,000 × *g*). The pellet was washed with 70% (vol/vol) ethanol, dried, and resuspended in 200 μL TE.

Expression and Purification of sHsps. For purification of heat shock protein (Hsp) 17.7 and Hsp20.2, N-terminal SUMO (small ubiquitin-like modifier) fusions were constructed. SUMO (1-98) was amplified from yeast genomic DNA and cloned via NdeI and BamHI into pET28b (Invitrogen), resulting in an N-terminal His6-tag. The hsp17.7 and hsp20.2 genes were amplified by PCR and cloned via BamHI and XhoI into pET28b behind the SUMO gene. *Escherichia coli* BL21 cells carrying the respective plasmid were cultured in LB media at 37 °C until an OD_{600} of 0.7 was reached. Expression was induced with 1 mM isopropyl-beta-D-thio-galactopyranoside (IPTG), and the cells were harvested after another 4 h by centrifugation (10 min, 5,000 × *g*). The pellet was resuspended in buffer A [40 mM sodium phosphate (pH 7.4), 300 mM NaCl, 40 mM imidazole) and lysed using a cell disruptor (BasicZ; Constant Systems). The small Hsps (sHsps) were purified from the resulting lysate by Ni^{2+}-chelating chromatography (GE Healthcare). The proteins were dialyzed against buffer A and cleaved with the His-tagged SUMO protease ubiquitin-like protease 1. The solution was applied to Ni^{2+}-chelating chromatography again, and the flow through was further purified on a 16/60 Sephacryl 300 HR gel filtration column (GE Healthcare) equilibrated in TE-50 [50 mM Tris·HCl (pH 7.4), 2 mM EDTA]. sHsp-containing fractions were pooled, flash-frozen in liquid nitrogen, and stored at −80 °C.

Preparation of Cell Lysates. *D. radiodurans* was grown in 2 × 50 mL TGY (1% bactotryptone, 0.5% yeast extract, and 0.1% glucose) for 72 h at 30 °C. The cells were resuspended in PBS containing 5 mM EDTA and protease inhibitors (Mix G; Serva) and lysed using a Retsch MM400 mixer mill.

Native PAGE. Proteins were separated by Native PAGE using 4–12% (vol/vol) Tris-Glycin precast gradient gels (Serva) according to the supplier's instructions. The Native Mark molecular weight standard (Invitrogen) was used for size determination.

Immunoblotting and Immunoprecipitation. Proteins were separated by SDS/PAGE and transferred to nitrocellulose membranes. The immunodetection was performed using polyclonal rabbit antiserum raised against purified Hsp17.7 or Hsp20.2 (Pineda). For detection, a horseradish peroxidase-linked secondary conjugate (Sigma) was used, and reactive bands were visualized by enhanced chemiluminescense (ECL-Plus) detection reagents (GE Healthcare).

For immunoprecipitation (IP), 200 μg of total protein of freshly prepared *D. radiodurans* lysates were incubated with 10 μg of purified sHsp for 30 min at 43 °C. Ten microliters of polyclonal rabbit antiserum was added subsequently, and the samples were incubated for 30 min at 20 °C and a further 30 min on ice. Twenty microliters of 50% (wt/vol) Protein G Sepharose slurry pre-equilibrated in IP buffer [25 mM Tris·HCl, 150 mM NaCl, 1 mM EDTA, 1% Nonidet P-40, and 5% (vol/vol) glycerol, pH 7.4] was added, and the samples were further incubated with agitation for 60 min on ice. The protein G Sepharose with attached complexes was sedimented by centrifugation (1 min, 500 × *g*) and washed four times with 500 μL IP buffer until no unspecific binding proteins were detected in these washing fractions. Complexed proteins were eluted using 50 μL Pierce Co-Immunoprecipitation Elution Buffer (pH 2.8, including primary amines) or SDS/PAGE loading buffer. Ten microliters of the eluate was separated by SDS/PAGE.

In Vivo Complementation Experiments. *D. radiodurans* sHsps were cloned into a modified pBad22 vector via NdeI and XbaI restriction sites. The overexpression plasmid for *ibpA/B* (pUHE21) and the *ibpA/B* knockout strain (MC4100) was a kind gift of A. Mogk (University of Heidelberg, Heidelberg, Germany). For comparison of final OD_{600} values, 3 mL cultures with and without 1 mM IPTG and 0.1% L-arabinose were inoculated with cells from stationary-phase liquid cultures and grown for 20 h at 37 °C. Cell suspensions were diluted 1:10 for recording of final OD_{600} values.

Isolation of aggregated protein was generally carried out as described elsewhere (1). Briefly, overnight cultures of *E. coli* were diluted to a final OD_{600} of 0.1 in LB media supplemented with 1 mM IPTG and 0.1% L-arabinose and were grown at 30 °C until they reached mid-exponential growth phase. Heat shock was carried out in a water bath (Julabo) at 46 °C for 30 min. Cells were cooled to 30 °C and recovered for 15 min at 30 °C. Afterward, cells were cooled rapidly in ice water, and 50 mL of the culture were harvested (10 min, 3,000 × *g* at 4 °C). Cells were resuspended according to their OD_{600} (1 mL of OD_{600} = 1 in 5 μL) in ice-cold buffer A [10 mM potassium phosphate (pH 6.5), 1 mM EDTA, 20% (wt/vol) sucrose, and 1 mg/mL lysozyme] and left on ice for 30 min. For cell lysis 100 μL of resuspended cells were diluted 1:10 into buffer B [10 mM potassium phosphate (pH 6.5) and 1 mM EDTA] and sonicated for 5 min. After removal of cell fragments, aggregated protein was pelleted and frozen in liquid nitrogen. Resuspended pellets were washed once with buffer B and twice with buffer B with 2% (vol/vol) Nonidet P-40 to remove lipids from the pellet. Finally aggregated proteins were resuspended and incubated for 5 min at 95 °C in SDS/PAGE loading buffer before separation by SDS/PAGE.

Analytical Ultracentrifugation. Sedimentation velocity experiments (SV-AUC) were carried out with a ProteomLab XL-I (Beckman) equipped with absorbance and interference optics. Four hundred microliters of the samples and 410 μL of the phosphate buffer were loaded into assembled cells with quartz windows and 12-mm path length charcoal-filled epon double sector centerpieces and were centrifuged at 42,000 rpm using an AN Ti-60 rotor (Beckman) for Hsp17.7 samples and an AN Ti-50 rotor for Hsp20.2 samples. The signal at 280 nm or 230 nm was monitored and one replicate was taken. Data analysis was carried out with the Ultrascan and the USLIMS platform (2). In brief, after 2D grid analysis and a Monte Carlo simulation (50 iterations), the data fit was further refined by a genetic algorithm and finally tested for robustness by another Monte Carlo simulation (50 iterations). Alternatively, the data were analyzed using the continuous c(S) distribution mode of sedfit (3, 4).

The multisignal ck(S) distribution was calculated with the multi-wavelength discrete/continuous distribution analysis of SEDPHAT

(5, 6) using an extinction coefficient of 4,470 $M^{-1}\cdot cm^{-1}$ for Hsp20.2 and 38,000 $M^{-1}\cdot cm^{-1}$ for lysozyme and a refractive index increment of 55,550 $M^{-1}\cdot cm^{-1}$ for Hsp20.2 and 46,750 $M^{-1}\cdot cm^{-1}$ for lysozyme, respectively.

For analysis of substrate complexes, Hsp17.7 was labeled with Alexa 488 succimidylester (Invitrogen) according to the manufacturer's protocol, and sedimentation was monitored in a ProteomLab XL-A (Beckman) ultracentrifuge equipped with a fluorescence detection system (AVIV Biomedical). For substrate binding analysis, 10 μM lysozyme in 100 nM sodium phosphate (pH 7.4) and 50 mM NaCl were incubated with increasing Hsp20.2 concentrations ranging from 0 to 40 μM Hsp20.2 in the presence of 1 mM Tris(2-carboxyethyl)phosphine (TCEP) for 1 h and subjected to analytical ultracentrifugation sedimentation velocity runs.

CD Spectroscopy. CD spectra were recorded using a Jasco J-715 spectropolarimeter with a PTC 343 peltier unit. The experiments were carried out in quartz cuvettetes with 0.1-cm path length. Thermal transitions were monitored at a constant wavelength of 220 nm with a heating rate of 20 °C per hour. Data were normalized by setting the signal of the unfolded protein to 1.

Protein Crystallization and Structure Determination. Crystals of Hsp17.7 were grown at 20 °C within 5 mo to their final size of 110 × 80 × 70 μm^3 by using the sitting drop vapor diffusion method. The drops contained equal volumes of protein (12 mg/mL) and reservoir solution [0.2 M ammoniumacetate, 0.1 M bis-Tris (pH 6.5), and 25% (wt/vol) PEG 3350]. Before exposure to X-rays, crystals were soaked in reservoir solution for 30 s and subsequently frozen in a stream of cold nitrogen gas at 100 K. A native dataset was collected on a Bruker Microstar/X8 Proteum (Bruker AXS) with a Cu rotating anode (λ = 1.54 Å) and processed with the Proteum software suite (Bruker AXS). Hsp17.7 crystallized in the trigonal space group P3121 with cell parameters of a,b = 51.3 Å, c = 80.5 Å.

For structure determination, molecular replacement was performed in Phaser (7) using the coordinates of HspA from *Xanthomonas sp.* (XAC1151; Protein Data Bank ID code 3GLA) as a starting model. The crystal structure of Hsp17.7 was completed in successive rounds with the interactive 3D graphic program MAIN (8). The model was refined with restraints between bonded atoms and between noncrystallographic symmetry-related atoms using TLS parameters and REFMAC5 (9), which yielded current crystallographic values of Rcryst = 0.197 and Rfree = 0.253. Coordinates were confirmed to have good stereochemistry from the Ramachandran plot, with 96% of residues in the most favored region and 4% of residues in the additionally allowed regions (Table S1). The asymmetric unit contains one subunit and 79 water molecules. The N-terminal 45 and the last 19 C-terminal amino acids are structurally disordered.

Mass Spectrometry and Bioinformatics. Commassie-stained lanes were sliced into four parts and treated as individual samples. Proteins were reduced, alkylated, and digested overnight with trypsin as described previously (10). Peptides were extracted in five steps by adding sequentially 200 μL of buffer A (water with 0.1% formic acid), acetonitrile (ACN), buffer A, ACN, ACN respectively. After each step, samples were treated for 15 min by sonication. After steps 2, 4, and 5 the supernatant was removed from the gel slices and collected for further processing.

The collected supernatants were pooled, concentrated in a speed vac (DNA120; Thermo Scientific) to ~20 μL end volume and filtered through a 0.22-μm centrifuge filter (Millipore). Peptides were loaded onto an Acclaim PepMap RSLC C18 trap column (Thermo Scientific) with 5 μL/min and separated on a PepMap RSLC C18 column (75 μm × 150 mm, C18, 2 μm, 100 A; Thermo Scientific) at a flow rate of 0.2 μL/min. A linear gradient from 5% (vol/vol) to 35% (vol/vol) buffer B (100% acetonitrile with 0.1% formic acid) eluted the peptides in 60 min to an LTQ Orbitrap XL (Thermo Scientific). Full scans and five dependent MS^2 scans (6 collision-induced dissociation or 3 collision-induced dissociation and 2 higher-energy C-trap dissociation spectra) were recorded in each cycle.

The mass spectrometry data derived from each gel slice were searched against a *D. radiodurans* database containing 3,167 proteins downloaded from the National Center for Biotechnology Informaiton (14.07.2011) using the SEQUEST algorithm implemented into the software "Proteome Discoverer 1.3" (Thermo Scientific). The search was limited to tryptic peptides containing a maximum of two missed cleavage sites, monoisotopic precursor ions, and a peptide tolerance of 10 ppm for precursors and 0.5 Da for fragment masses. Proteins were identified with two distinct peptides with a target false discovery rate for peptides below 1% according to the decoy search. Proteins also detected in control experiments using rabbit preimmune-sera in the IP reaction were manually removed.

Electron Microscopy and Image Processing. For negative stain electron microscopy, 5 μL of the protein sample (0.05 mg/mL protein in 50 mM Hepes/KOH, 75 mM NaCl, pH 7.4) were adsorbed for 2 min onto carbon-coated grids that were glow discharged in air. Excess solution was blotted off, and the samples were negatively stained for 30 s using uranyl acetate [1.5% (wt/vol) at pH 4.5]. Electron micrographs were recorded at a calibrated magnification of 58,000 and at defocus values of 400–1,000 nm using a JEOL JEM 100CX electron microscope operated at 100 kV. Suitable micrographs were digitized at a step size of 8.5 μm using a FlexTight X5 array scanner, resulting in a pixel size of 1.46 Å at the specimen level.

Well-separated single particle images on electron micrographs were semimanually selected using Boxer from the Eman software package (11), which was also used for the determination of the defoci and the correction of contrast transfer function (CTF) by phase flipping. The following image processing procedures were carried out using the Imagic suite (12). In a first step, CTF-corrected molecular images from several micrographs were pooled, band-pass filtered between 10 and 170 Å, and normalized. Translational alignment was performed by mass centering. Upon multivariate statistical analysis, class averaging has been performed. For an estimation of the oligomeric size distributions, the circumscribing diameters of all class averages for each sample have been measured.

Multiple Sequence Alignment. Multiple alignments of sequences have been calculated using the CLUSTAL Web server and default parameters. The alignment of the Hsp17.7 β10-strand was improved manually on the basis of the crystal structure.

1. Tomoyasu T, Mogk A, Langen H, Goloubinoff P, Bukau B (2001) Genetic dissection of the roles of chaperones and proteases in protein folding and degradation in the *Escherichia coli* cytosol. *Mol Microbiol* 40(2):397–413.
2. Brookes E, Cao W, Demeler B (2010) A two-dimensional spectrum analysis for sedimentation velocity experiments of mixtures with heterogeneity in molecular weight and shape. *Eur Biophys J* 39(3):405–414.
3. Schuck P (2000) Size-distribution analysis of macromolecules by sedimentation velocity ultracentrifugation and lamm equation modeling. *Biophys J* 78(3):1606–1619.
4. Schuck P, Perugini MA, Gonzales NR, Howlett GJ, Schubert D (2002) Size-distribution analysis of proteins by analytical ultracentrifugation: Strategies and application to model systems. *Biophys J* 82(2):1096–1111.
5. Balbo A, et al. (2005) Studying multiprotein complexes by multisignal sedimentation velocity analytical ultracentrifugation. *Proc Natl Acad Sci USA* 102(1):81–86.
6. Padrick SB, et al. (2010) Determination of protein complex stoichiometry through multisignal sedimentation velocity experiments. *Anal Biochem* 407(1):89–103.
7. McCoy AJ, et al. (2007) Phaser crystallographic software. *J Appl Cryst* 40(Pt 4): 658–674.

8. Turk D (1992) Improvement of a programme for molecular graphics and manipulation of electron densities and its application for protein structure determination. PhD thesis (Technische Universität München, Munich).
9. Vagin AA, et al. (2004) REFMAC5 dictionary: Organization of prior chemical knowledge and guidelines for its use. *Acta Crystallogr D Biol Crystallogr* 60(Pt 12 Pt 1):2184–2195.
10. Haslbeck M, et al. (2004) Hsp42 is the general small heat shock protein in the cytosol of Saccharomyces cerevisiae. *EMBO J* 23(3):638–649.
11. Ludtke SJ, Baldwin PR, Chiu W (1999) EMAN: Semiautomated software for high-resolution single-particle reconstructions. *J Struct Biol* 128(1):82–97.
12. van Heel M, Harauz G, Orlova EV, Schmidt R, Schatz M (1996) A new generation of the IMAGIC image processing system. *J Struct Biol* 116(1):17–24.

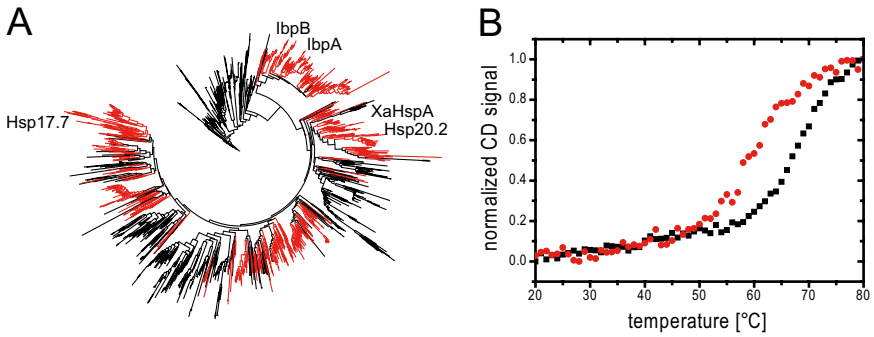

Fig. S1. Evolutionary distance and protein stability of Hsp17.7 and Hsp20.2. (*A*) The evolutionary distance of Hsp17.7 and Hsp20.2. A phylogenetic tree of the family of sHsps adopted according to Kriehuber et al. (1) is shown. Bacteria are colored in red and all other phyla in black. The position of the sHsps of *E. coli* (IbpA; IbpB), *Xanthomonas spec*. (XaHspA), and *D. radiodurans* (Hsp20.2, Hsp17.7) is indicted. (*B*) Stability of *D. radiodurans* sHsps. Thermal transition of Hsp17.7 and Hsp20.2. Protein concentration, 10 μM. Temperature-induced changes in the far-UV CD signal of Hsp17.7 (black) and Hsp20.2 (red) were monitored at a constant wavelength of 220 nm.

1. Kriehuber T, et al. (2010) Independent evolution of the core domain and its flanking sequences in small heat shock proteins. *FASEB J* 24(10):3633–3642.

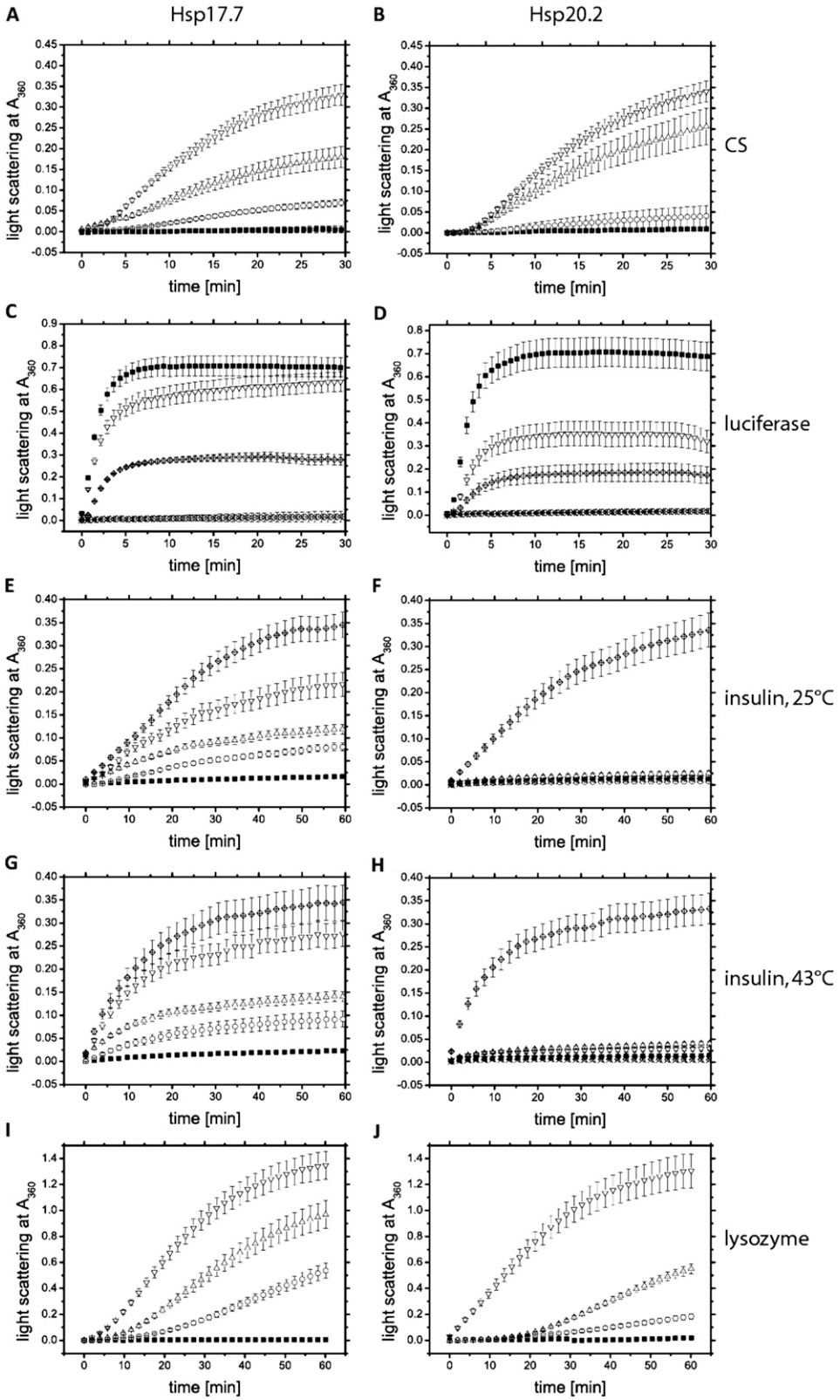

Fig. S2. Chaperone activity of Hsp17.7 and Hsp20.2. Chaperone function was assessed by the ability to suppress the aggregation of CS, luciferase, insulin, and lysozyme. The kinetic of aggregation was determined after the light scattering of the samples at 360 nm. All assays were performed in triplicates, and mean values and the respective SDs (error bars) are indicated. (*A*) Influence of Hsp17.7 on the thermal aggregation of CS. CS (final concentration: 150 nM monomer) was diluted into a thermostated solution (43 °C) of 300 nM (△), 600 nM (○), and 3 μM (■) Hsp17.7 monomer. ▽ represent the spontaneous aggregation of CS at 43 °C. (*B*) Thermal CS (final concentration: 150 nM monomer) aggregation was monitored at 360 nm in a UV/Vis spectrophotometer in the absence (▽) and presence of of 150 nM (△), 300 nM (○), and 600 nM (■) Hsp20.2 monomer. (*C*) Influence of Hsp17.7 on the thermal aggregation of luciferase. Luciferase (final

Legend continued on following page

concentration: 1 μM monomer) was diluted into a thermostated solution (43 °C) of 1 μM (▽), 5 μM (◇), and 10 μM (□) Hsp17.7 monomer. ■ represents the spontaneous aggregation of luciferase at 43 °C. (*D*) Thermal denaturation of luciferase in the presence of Hsp20.2. luciferase (final concentration: 1 μM monomer) was diluted into a thermostated solution (43 °C) of 1 μM (▽), 2 μM (◇), and 5 μM (□) Hsp20.2 monomer. ■ represents the spontaneous aggregation of luciferase at 43 °C. (*E*) Influence of Hsp17.7 on the aggregation of insulin upon reduction with DTT. Insulin (final concentration: 50 μM monomer) was diluted into a thermostated solution (25 °C) of 1 μM (▽), 2 μM (◇), 4 μM (○), and 16 μM (■) Hsp17.7 monomer. ◇ represents the spontaneous aggregation of insulin at a final concentration of 20 mM DTT. (*F*) Influence of Hsp20.2 on the aggregation of insulin upon reduction with DTT. Insulin (final concentration: 50 μM monomer) was diluted into a thermostated solution (25 °C) of 1 μM (▽), 2 μM (◇), 4 μM (○), and 16 μM (■) Hsp20.2 monomer. ◇ represents the spontaneous aggregation of insulin at a final concentration of 20 mM DTT. (*G*) Influence of Hsp17.7 on the aggregation of insulin upon reduction with DTT. Insulin (final concentration: 50 μM monomer) was diluted into a thermostated solution (43 °C) of 1 μM (▽), 2 μM (△), 4 μM (○), and 16 μM (■) Hsp17.7 monomer. ◇ represents the spontaneous aggregation of insulin at a final concentration of 20 mM DTT. (*H*) Influence of Hsp20.2 on the aggregation of insulin upon reduction with DTT. Insulin (final concentration: 50 μM monomer) was diluted into a thermostated solution (43 °C) of 1 μM (▽), 2 μM (△), 4 μM (○), and 16 μM (■) Hsp20.2 monomer. ◇ represents the spontaneous aggregation of insulin at a final concentration of 20 mM DTT. (*I*) Influence of Hsp17.7 on the aggregation of lysozyme upon reduction with TCEP. Lysozyme (final concentration: 1 μM monomer) was diluted into a thermostated solution (25 °C) of 2 μM (△), 4 μM (○), and 16 μM (■) Hsp17.7 monomer. ▽ represents the spontaneous aggregation of insulin at a final concentration of 1 mM TCEP. (*J*) Influence of Hsp20.2 on the aggregation of lysozyme upon reduction with TCEP. Lysozyme (final concentration: 1 μM monomer) was diluted into a thermostated solution (25 °C) of 2 μM (△), 4 μM (○), and 16 μM (■) Hsp20.2 monomer. ▽ represents the spontaneous aggregation of insulin at a final concentration of 1 mM TCEP.

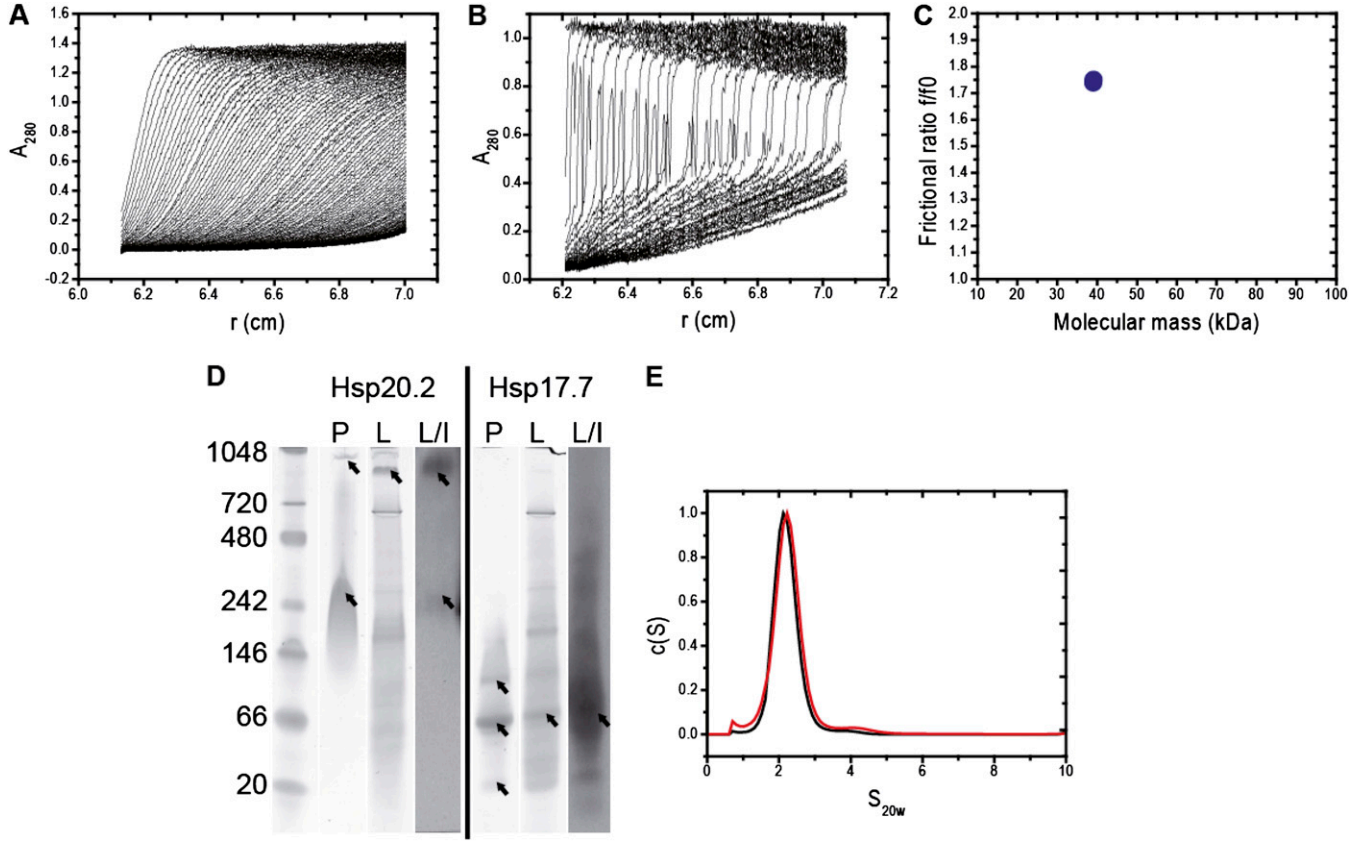

Fig. S3. Quaternary structure of Hsp17.7 and Hsp20.2. (*A* and *B*) analytical ultracentrifugation sedimentation profile of Hsp17.7 (*A*) at 1.0 mg/mL and Hsp20.2 (*B*) at 1.5 mg/mL. (*C*) Pseudo-3D visualization of the global fit result (2D grid analysis and genetic algorithm). The graph displays the molecular weight of Hsp17.7 (*x* axis), the frictional ratio (f/f0) (*y* axis), and the partial concentration as intensity. (*D*) Analysis of the molecular mass of the *D. radiodurans* sHsps by native PAGE. Ten micrograms of the purified *D. radiodurans* sHsps (lane P) as well as freshly prepared cellular lysate of *D. radiodurans* (100 μg total protein) after addition of 5 μg purified sHsp were separated by native PAGE (lane L). To verify the position of the sHsps in the background of the lysate, immunoblot analysis of the respective lanes was performed (lanes L/I). Arrows highlight the respective bands corresponding to the sHsps. (*E*) Analysis of the formation of hetero-oligomers of Hsp20.2 and Hsp17.7. Hsp17.7 was labeled with Alexa 488, and multisignal sedimentation velocity analysis was performed. c(S) distribution of 1 μM Hsp17.7-Alexa488 (black) and 10 μM Hsp17.7-Alexa488 + 100 μM Hsp20.2 (red).

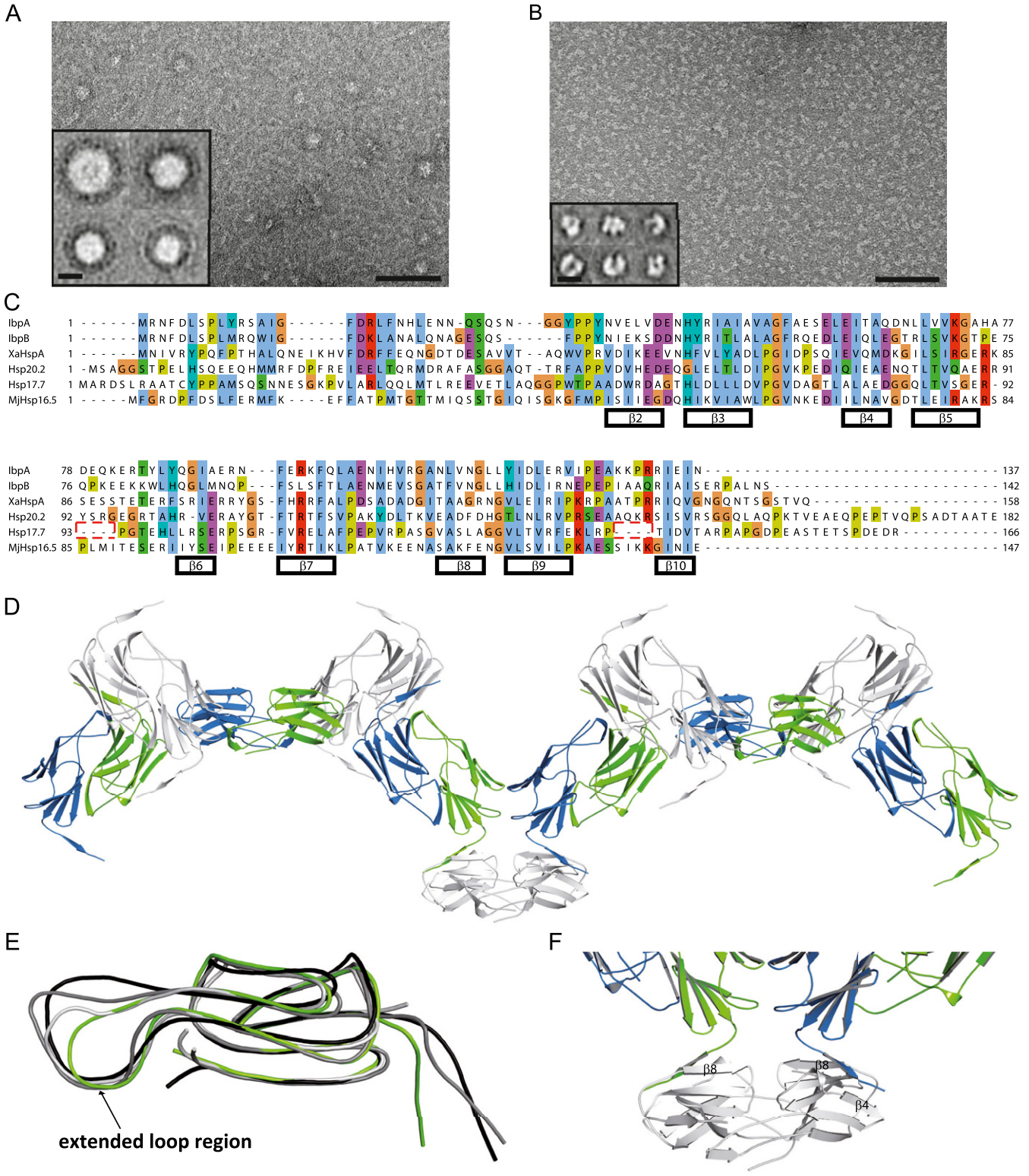

Fig. S4. Structure of Hsp17.7 and Hsp20.2. (*A* and *B*) Characteristic transmission electron microscopy micrographs of negatively stained Hsp20.2 (*A*) and Hsp17.7 (*B*) at 0.05 mg/mL protein in 1.5% (wt/vol) uranyl acetate. (Scale bar, 100 nm.) (*Insets*) Characteristic class averages of the oligomers or dimers, respectively. (Scale bar, 10 nm.) (*C*) Multiple sequence alignment of Hsp17.7, Hsp20.2, IbpA/B, MjHsp16.5, and XaHspA. The β-sheets formed in the Hsp17.7 crystal are indicated. Red boxes mark peculiar gaps in the Hsp17.7 sequence. (*D*) Crystal packing of Hsp17.7. The dimer building blocks are assembled in a helical, lined-up order owing to the trigonal space group. (*E*) Backbone superposition of one monomer of Hsp17.7 (green), XaHspA (light gray), MjHSP16.5 (dark gray), and TaHSP16.9 (black). The comparison of the superimposed backbones exhibits significant structural variations for the extended loop region. (*F*) Close up of the C-terminal extensions of Hsp17.7 monomers (blue and green, respectively) containing the conserved IXI/V-motif, which adopts β-strand conformation (β10 strand) by binding in a hydrophobic groove formed by the β4 and β8 strands of an adjacent monomer (light gray).

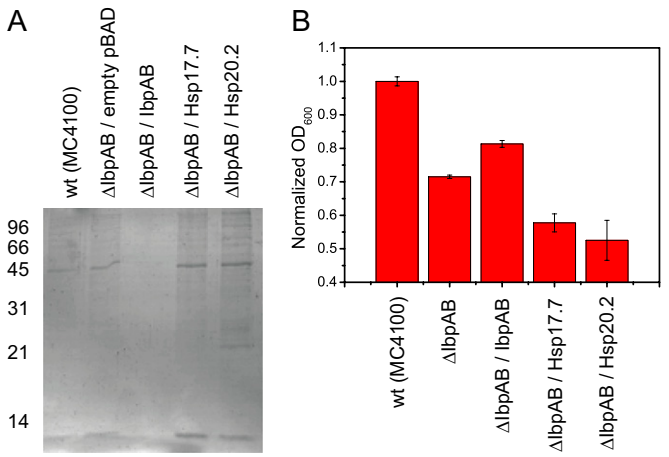

Fig. S5. Complementation of IbpA/B deletion with *D. radiodurans* sHsps. (*A*) SDS/PAGE of aggregates isolated from WT and ΔibpA/B strains transfected with either empty plasmid or plasmids overexpressing IbpA/B, Hsp17.7, or Hsp20.2 after heat shock at 30 min at 45 °C followed by 15 min of recovery at 30 °C (1). (*B*) Complementation of a ΔibpA/B strains by plasmid-based expression of IbpA/B, Hsp17.7, and Hsp20.2. Normalized OD_{600} (average ± SD) of *E. coli* cells grown to stationary phase at 37 °C.

1. Tomoyasu T, Mogk A, Langen H, Goloubinoff P, Bukau B (2001) Genetic dissection of the roles of chaperones and proteases in protein folding and degradation in the *Escherichia coli* cytosol. *Mol Microbiol* 40(2):397–413.

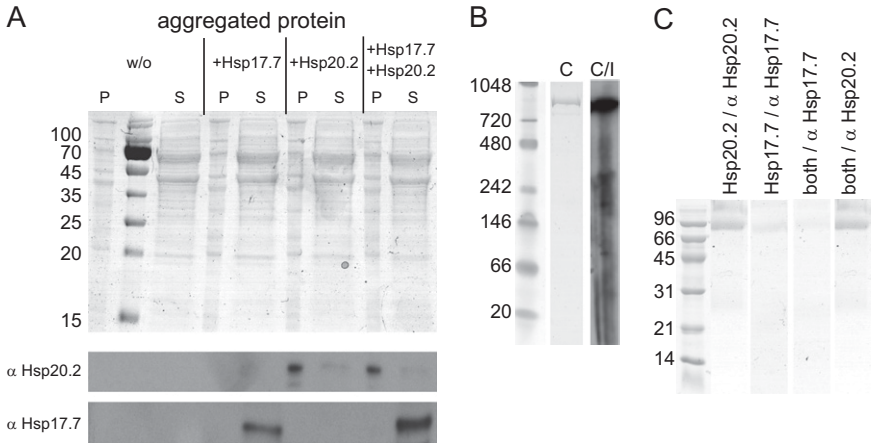

Fig. S6. Analysis of substrate binding of *D. radiodurans* sHsps. (*A*) Lysates of logarithmically growing *D. radiodurans* cells at 30 °C were prepared. Two hundred micrograms of total lysate protein was heat stressed for 30 min at 43 °C without (w/o) or with addition of 10 μg of Hsp20.2 and/or Hsp17.7. After incubation, the aggregated protein was separated by centrifugation (10 min, 10,000 × *g*), and the samples were analyzed by SDS/PAGE and immunoblot. (*B*) Samples with added Hsp20.2 were treated as described in *A*, and resulting pellet including sHsp–substrate complexes were analyzed by native page (lane C) and immunoblotting (lane C/I). The major high molecular weight band, detected by immunoblot (arrow) was excised and analyzed by MS. (C) sHsp–substrate complexes were isolated by IP, and the resulting elution fractions were separated by SDS/PAGE. The respective proteins in the IPs were identified by MS analysis excising the complete lane in three parts.

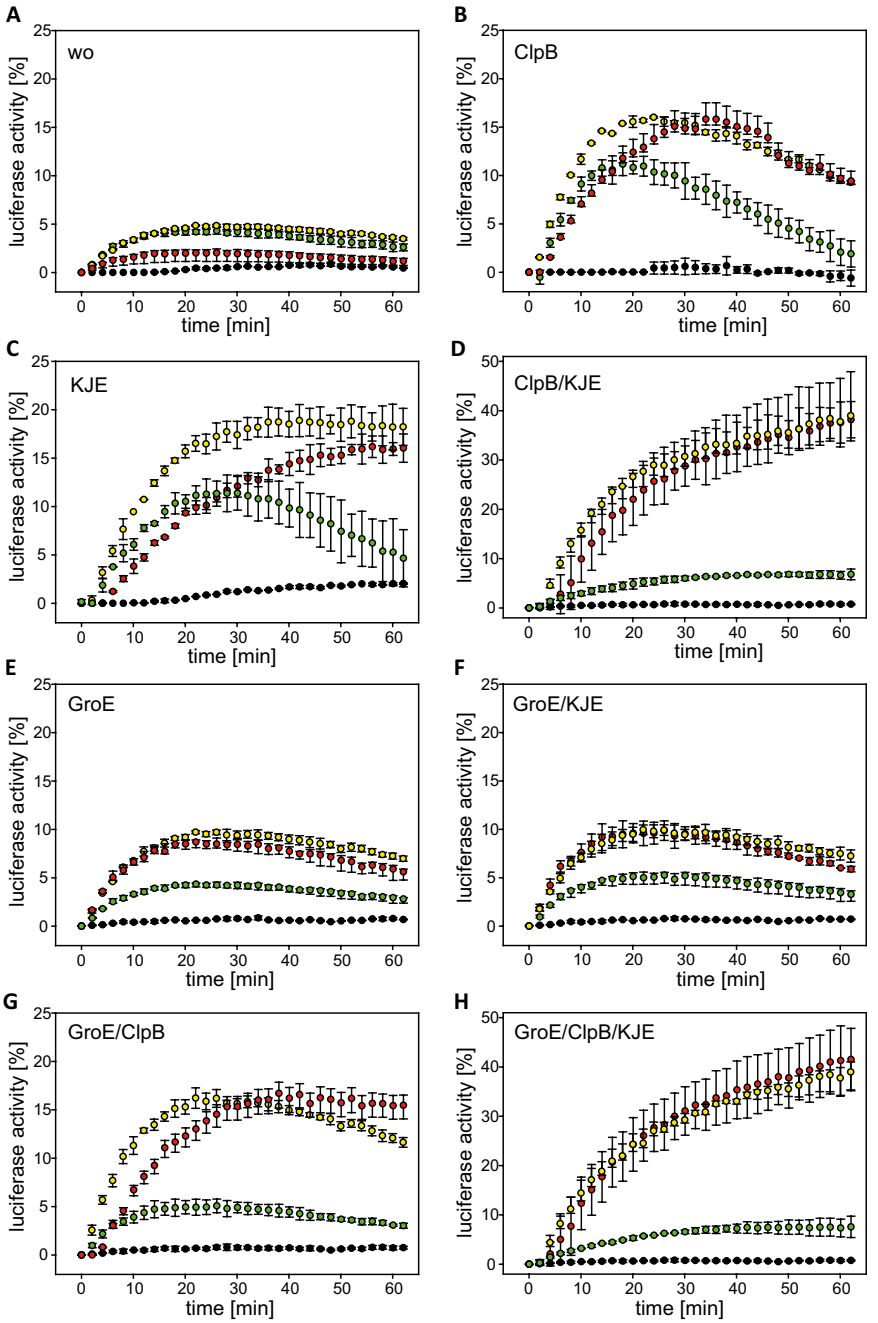

Fig. S7. Analysis of luciferase release from Hsp17.7 and Hsp20.2. Effects of Hsp17.7 and Hsp20.2 on the refolding efficiency of heat-denatured luciferase by the KJE, ClpB, and GroE chaperone machineries. Luciferase (80 nM) was incubated at 43 °C for 10 min in the absence (black) of sHsps or in the presence of 600 nM Hsp20.2 (red), 600 nM Hsp17.7 (green), or 600 nM of Hsp20.2 and Hsp17.7 (yellow). Luciferase activity was followed kinetically for 65 min. Assays were performed in triplicates; mean values and the respective SD are indicated. For normalization, the activity of 80 nM untreated luciferase was set to 100%. After complete inactivation, the samples were shifted to 25 °C, and subsequently different mixtures of chaperones were added. (*A*) Without addition of further chaperones. (*B*) Addition of ClpB (600 nM). (*C*) Addition of DnaK/DnaJ/GrpE (KJE, 0.6, 1.2, and 0.6 μM). (*D*) Addition of ClpB (600 nM) and DnaK/DnaJ/GrpE (KJE, 0.6, 1.2, and 0.6 μM). (*E*) Addition of GroE (600 nM GroEL and GroES). (*F*) Addition of GroE (600 nM GroEL and GroES) and DnaK/DnaJ/GrpE (KJE, 0.6, 1.2, and 0.6 μM). (*G*) Addition of GroE (600 nM GroEL and GroES) and ClpB (600 nM). (*H*) Addition of GroE (600 nM GroEL and GroES), ClpB (600 nM), and DnaK/DnaJ/GrpE (KJE, 0.6, 1.2, and 0.6 μM).

Table S1. Data collection and refinement statistics

Parameter	Dr_sHSP17.7*
Crystal parameters	
Space group	$P3_121$
Cell constants	a,b = 51,3 Å, c = 80.4 Å,
Data collection	
Rotating anode	CuK_α
Wavelength (Å)	1.5418
Resolution range (Å)†	40–2.4 (2.5–2.4)
No. observations	87023
No. unique reflections‡	5119
Completeness (%)†	99.9 (100.0)
R_{merge} (%)†,§	5.3 (36.9)
I/σ (I)†	18.4 (5.3)
Refinement (REFMAC5)	
Resolution range (Å)	15–2.4
No. reflections working set	4539
No. reflections test set	209
No. non hydrogen	757
No. of solvent water	79
R_{work}/R_{free} (%)¶	19.7/25.3
rmsd bond lengths (Å)/(°)‖	0.017/1.54
Average B-factor (Å^2)	25.8
Ramachandran Plot (%)**	96.0/4.0/0.0

*Dataset has been collected on a single crystal.

†The values in parentheses of resolution range, completeness, R_{merge}, and I/σ (I) correspond to the last resolution shell.

‡Friedel pairs were treated as different reflections.

§$R_{merge}(I) = \Sigma_{hkl}\Sigma_j |[I(hkl)_j - I(hkl)]|/[\Sigma_{hkl} I_{hkl}]$, where $I(hkl)_j$ is the j^{th} measurement of the intensity of reflection hkl and <I(hkl)> is the average intensity.

¶$R = \Sigma_{hkl} || F_{obs}| - |F_{calc}| |/\Sigma_{hkl} |F_{obs}|$, where R_{free} is calculated without a sigma cutoff for a randomly chosen 5% of reflections, which were not used for structure refinement, and R_{work} is calculated for the remaining reflections.

‖Deviations from ideal bond lengths/angles.

**Number of residues in favored region/allowed region/outlier region.

Table S2. Proteins identified by mass spectrometry

Accession	Gene locus	Description	20	17/20	Agg	MM (kDa)	Calc. pI
NP_295836.1	DR_2113	30S ribosomal protein S5	34.32	6.60	9.03	21.0	10.35
NP_295833.1	DR_2110	30S ribosomal protein S8	10.55	5.07	11.00	15.0	10.05
NP_295768.1	DR_2045	50S ribosomal protein L1	15.69	9.56	7.04	24.3	9.55
NP_294046.1	DR_0323	50S ribosomal protein L5	18.61	9.25	9.28	20.3	9.88
NP_295203.1	DR_1480	AlgP-like protein	63.48	13.51	94.67	55.9	8.78
NP_294838.1	DR_1114	HSP20 family protein	49.33	48.49	9.27	20.2	5.10
NP_293941.1	DR_0217	Thiosulfate sulfurtransferase	44.35	15.80	6.35	32.2	4.98
NP_293809.1	DR_0083	2-Oxoglutarate dehydrogenase, dihydrolipoamide succinyltransferase E2 component	9.78	13.00	0.00	44.5	5.34
NP_295236.1	DR_1513	30S ribosomal protein S2	27.05	14.05	0.00	29.7	5.62
NP_295850.1	DR_2127	30S ribosomal protein S4	27.29	11.02	0.00	23.8	10.37
NP_294029.1	DR_0306	30S ribosomal protein S7	18.11	7.96	0.00	17.9	10.58
NP_294039.1	DR_0316	50S ribosomal protein L22	15.03	9.88	0.00	15.1	10.74
NP_294035.1	DR_0312	50S ribosomal protein L4	9.21	8.92	0.00	22.3	9.48
NP_295830.1	DR_2107	ABC transporter ATP-binding protein	6.09	11.28	0.00	28.0	4.98
NP_295695.1	DR_1972	ATP-dependent Clp protease proteolytic subunit	12.58	6.78	0.00	23.0	5.19
NP_296307.1	DR_2588	Iron ABC transporter periplasmic substrate-binding protein	3.57	2.89	0.00	36.3	9.77
NP_051655.1	DR_B0125	Iron ABC transporter, periplasmic substrate-binding protein	8.93	8.07	0.00	35.1	9.72
NP_296355.1	DR_2637	Phosphopyruvate hydratase	16.85	6.60	0.00	45.5	5.02
NP_294466.1	DR_0743	Response regulator	12.45	6.31	0.00	25.4	5.25
NP_294040.1	DR_0317	30S ribosomal protein S3	7.99	0.00	6.22	27.3	10.98
NP_294037.1	DR_0314	50S ribosomal protein L2	10.46	0.00	6.78	30.0	11.08
NP_295443.1	DR_1720	Aconitate hydratase	32.26	0.00	25.99	97.9	5.07
NP_296082.1	DR_2361	Acyl-CoA dehydrogenase	28.55	0.00	2.88	66.2	5.44
NP_294923.1	DR_1199	Protease I	7.86	0.00	5.59	20.7	5.05
NP_293980.1	DR_0257	Pyruvate dehydrogenase subunit E1	8.92	0.00	58.18	104.1	5.45
NP_295848.1	DR_2125	30S ribosomal protein S13	9.13	0.00	0.00	14.2	11.00
NP_294043.1	DR_0320	30S ribosomal protein S17	5.90	0.00	0.00	10.8	9.70
NP_293827.1	DR_0101	30S ribosomal protein S18	6.00	0.00	0.00	10.6	11.39
NP_293899.1	DR_0175	30S ribosomal protein S9	7.64	0.00	0.00	14.7	11.17
NP_296197.1	DR_2477	3-Hydroxyacyl-CoA dehydrogenase	11.52	0.00	0.00	84.7	6.19
NP_293898.2	DR_0174	50S ribosomal protein L13	10.13	0.00	0.00	16.3	9.99
NP_294044.1	DR_0321	50S ribosomal protein L14	6.85	0.00	0.00	14.2	10.86
NP_295838.1	DR_2115	50S ribosomal protein L15	12.58	0.00	0.00	16.9	10.42
NP_294041.1	DR_0318	50S ribosomal protein L16	9.65	0.00	0.00	16.2	10.11
NP_295835.1	DR_2112	50S ribosomal protein L18	6.56	0.00	0.00	12.1	11.02
NP_294479.1	DR_0755	50S ribosomal protein L19	9.97	0.00	0.00	18.3	10.55
NP_295727.1	DR_2004	50S ribosomal protein L20	13.16	0.00	0.00	13.9	11.81
NP_294150.1	DR_0427	50S ribosomal protein L25/general stress protein Ctc	6.40	0.00	0.00	27.0	4.65
NP_294034.1	DR_0311	50S ribosomal protein L3	13.52	0.00	0.00	22.4	10.54
NP_295834.2	DR_2111	50S ribosomal protein L6	14.46	0.00	0.00	19.6	10.04
NP_295683.1	DR_1960	Acetyl-CoA acetyltransferase	2.99	0.00	0.00	41.1	5.72
NP_296200.1	DR_2480	Acetyl-CoA acetyltransferase	19.06	0.00	0.00	40.8	5.30
NP_296021.1	DR_2300	Alanyl-tRNA synthetase	14.59	0.00	0.00	95.9	5.43
NP_295748.1	DR_2025	ArgE/DapE/Acy1 family protein	6.31	0.00	0.00	49.6	5.07
NP_294072.1	DR_0349	ATP-dependent protease LA	5.67	0.00	0.00	90.3	5.95
NP_294353.1	DR_0630	Cell division protein FtsA	7.27	0.00	0.00	54.2	6.00
NP_294354.1	DR_0631	Cell division protein FtsZ	30.13	0.00	0.00	38.9	4.93
NP_051551.1	DR_B0008	Cob(I)alamin adenosyltransferase	12.22	0.00	0.00	23.4	6.81
NP_293961.1	DR_0237	Cyclophilin-type peptidyl-prolyl cis-trans isomerase	9.22	0.00	0.00	21.3	6.33
NP_294630.1	DR_0906	DNA gyrase subunit B	5.96	0.00	0.00	73.1	6.51
NP_295430.1	DR_1707	DNA-directed DNA polymerase	43.63	0.00	0.00	105.6	5.31
NP_295851.1	DR_2128	DNA-directed RNA polymerase subunit alpha	23.69	0.00	0.00	37.2	4.93
NP_294636.1	DR_0912	DNA-directed RNA polymerase subunit beta	40.75	0.00	0.00	131.0	5.41

Table S2. Cont.

Accession	Gene locus	Description	20	17/20	Agg	MM (kDa)	Calc. pI
NP_294635.1	DR_0911	DNA-directed RNA polymerase subunit beta'	39.89	0.00	0.00	171.3	5.35
NP_294694.1	DR_0970	Electron transfer flavoprotein subunit alpha	26.10	0.00	0.00	32.7	4.91
NP_294030.1	DR_0307	Elongation factor G	17.90	0.00	0.00	76.7	5.10
NP_295312.1	DR_1589	Fructose-bisphosphate aldolase	15.48	0.00	0.00	32.4	5.77
NP_295651.1	DR_1928	Glycerol kinase	6.61	0.00	0.00	55.0	5.48
NP_294922.1	DR_1198	GTP-binding elongation factor family protein TypA/BipA	11.90	0.00	0.00	66.0	5.25
NP_296029.1	DR_2308	GTP-binding protein EngA	22.89	0.00	0.00	49.5	5.69
NP_295263.1	DR_1540	Isocitrate dehydrogenase	20.36	0.00	0.00	47.4	5.25
NP_294806.1	DR_1082	Light-repressed protein A	8.83	0.00	0.00	22.0	6.15
NP_296313.1	DR_2594	Magnesium protoporphyrin chelatase	24.74	0.00	0.00	53.2	5.15
NP_294048.1	DR_0325	Malate dehydrogenase	12.05	0.00	0.00	35.1	5.24
NP_285600.1	DR_A0277	Malate synthase	21.32	0.00	0.00	58.5	5.47
NP_294284.1	DR_0561	Maltose ABC transporter periplasmic maltose-binding protein	7.80	0.00	0.00	41.8	9.69
NP_296227.1	DR_2507	Medium-chain fatty acid–CoA ligase	6.46	0.00	0.00	63.8	5.60
NP_294674.1	DR_0950	NADH dehydrogenase II	10.74	0.00	0.00	41.3	7.66
NP_295691.1	DR_1968	Nitroreductase	7.55	0.00	0.00	23.8	6.11
NP_295291.1	DR_1568	Peptide ABC transporter ATP-binding protein	14.57	0.00	0.00	42.0	6.86
NP_296107.1	DR_2386	Phenylacetate-CoA oxygenase subunit PaaA	13.64	0.00	0.00	36.6	5.77
NP_296105.1	DR_2384	Phenylacetic acid degradation protein PaaC	2.62	0.00	0.00	29.3	5.14
NP_285481.1	DR_A0157	Phosphate ABC transporter periplasmic phosphate-binding protein	8.03	0.00	0.00	42.0	9.82
NP_294701.1	DR_0977	Phosphoenolpyruvate carboxykinase	8.03	0.00	0.00	53.3	5.44
NP_294298.2	DR_0575	Preprotein translocase subunit SecA	22.38	0.00	0.00	97.2	5.19
NP_296296.1	DR_2576	Putative manganese-dependent inorganic pyrophosphatase	9.43	0.00	0.00	34.0	4.89
NP_293979.1	DR_0256	Pyruvate dehydrogenase complex, dihydrolipoamide acetyltransferase E2 component	10.21	0.00	0.00	63.6	5.05
NP_296091.1	DR_2370	Pyruvate dehydrogenase complex, dihydrolipoamide dehydrogenase E3 component	20.10	0.00	0.00	49.2	5.90
NP_294076.1	DR_0353	Ribonuclease	8.39	0.00	0.00	84.7	6.11
NP_296095.1	DR_2374	Ribonucleoside-diphosphate reductase-like protein	4.28	0.00	0.00	152.8	6.35
NP_294476.1	DR_0752	Septum site-determining protein	9.51	0.00	0.00	29.4	5.07
NP_293764.1	DR_0038	Serine hydroxymethyltransferase	10.24	0.00	0.00	47.4	6.81
NP_295182.1	DR_1459	Serine protease	19.57	0.00	0.00	63.5	9.00
NP_294972.1	DR_1248	Succinyl-CoA synthetase subunit alpha	8.95	0.00	0.00	30.9	5.68
NP_294971.1	DR_1247	Succinyl-CoA synthetase subunit beta	6.16	0.00	0.00	41.7	5.48
NP_294668.1	DR_0944	Thioredoxin	6.53	0.00	0.00	15.3	7.14
NP_295977.1	DR_2256	Transketolase	6.71	0.00	0.00	71.5	5.96
NP_295522.1	DR_1799	Translation initiation factor IF-2	22.77	0.00	0.00	64.0	4.98
NP_295810.1	DR_2087	Translation initiation factor IF-3	7.96	0.00	0.00	23.6	9.14
NP_296353.1	DR_2634	Tyrosyl-tRNA synthetase	8.33	0.00	0.00	45.5	6.28
NP_294423.1	DR_0700	V-type ATP synthase subunit A	13.77	0.00	0.00	63.5	5.00
NP_294424.1	DR_0701	V-type ATP synthase subunit B	11.21	0.00	0.00	51.3	5.34
NP_294425.1	DR_0702	V-type ATP synthase subunit D	8.06	0.00	0.00	23.9	9.44
NP_285329.1	DR_A0005	Zinc-containing alcohol dehydrogenase	27.64	0.00	0.00	42.0	6.52
NP_294010.1	DR_0287	2-Oxoglutarate dehydrogenase E1 component	0.00	0.00	4.68	105.9	5.81
NP_294128.1	DR_0405	α-Dextran endo-1,6-alpha-glucosidase	0.00	0.00	2.67	97.9	7.34
NP_295911.1	DR_2188	Aminopeptidase	0.00	0.00	7.74	45.7	5.24
NP_285582.1	DR_A0259	Catalase	0.00	0.00	5.68	84.0	6.92
NP_296230.1	DR_2510	Enoyl-CoA hydratase	0.00	0.00	5.17	28.3	5.67
NP_295756.1	DR_2033	Glutamine synthase	0.00	0.00	5.63	86.9	5.76
NP_294102.1	DR_0379	Outer membrane protein	0.00	0.00	67.02	90.2	6.15

A total of 118 proteins from *D. radiodurans* were identified either in triplicates of IP or native gels (Agg) (Fig. S5) as substrates of Hsp20.2. Seventeen proteins annotated as hypothetical have been excluded. For proteins that were identified by more than one experiment, the maximum score is indicated. Pink shading indicates the presence of the respective protein in the sample. Calc. pI, theoretical pI as calculated by Proteome Discoverer, MM, molecular mass. Accession numbers and locus tags refer to NCBI database (http://www.ncbi.nlm.nih.gov/).